Blind Carrier Frequency Offset Estimation in SISO, MIMO, and Multiuser OFDM Systems

Yingwei Yao, *Member, IEEE,* and Georgios B. Giannakis, *Fellow, IEEE*

Abstract—Relying on a kurtosis-type criterion, we develop a low-complexity blind carrier frequency offset (CFO) estimator for orthogonal frequency-division multiplexing (OFDM) systems. We demonstrate analytically how identifiability and performance of this blind CFO estimator depend on the channel's frequency selectivity and the input distribution. We show that this approach can be applied to blind CFO estimation in multi-input multi-output and multiuser OFDM systems. The issues of channel nulls, multiuser interference, and effects of multiple antennas are addressed analytically, and tested via simulations.

Index Terms—Carrier frequency offset (CFO), kurtosis, Multi-input multi-output orthogonal frequency-division multiplexing (MIMO-OFDM), multiuser OFDM, orthogonal frequency-division multiplexing (OFDM).

I. INTRODUCTION

ORTHOGONAL frequency-division multiplexing (OFDM) has found applications in various digital communication systems, such as digital audio/video broadcasting (DAB/DVB) and wireless local area networks (WLANs). Compared with single-carrier systems, OFDM is more sensitive to carrier frequency offsets (CFOs), so accurate estimation and compensation of CFO is very important [23].

Most CFO estimators rely on periodically transmitted pilots [20], [25]. However, pilot-assisted methods are less attractive for continuous-transmission OFDM-based systems, such as DAB and DVB. Along with the potential benefit of improving spectral efficiency, this motivates blind CFO estimation in commercial systems. Furthermore, in noncooperative (e.g., tactical) links, blind estimators are the only option, since training-based ones cannot even be implemented. One class of blind CFO estimators takes advantage of null subcarriers existing in many OFDM systems [2], [11], [14], [17]. These estimators are robust against channel multipath, but have relatively high computational costs. On the other hand, blind estimators using the cyclic prefix (CP) or the cyclostationarity (CS) of OFDM transmissions [4], [12], [13], [29] have lower complexity, but their performance degrades as frequency selectivity becomes more pronounced. The CP-based scheme proposed in [16] is robust against channel multipath, but requires that the CP is strictly longer than the channel delay spread, and that the exact channel order is known.

Multi-input multi-output (MIMO) systems, which rely on multiple antennas to provide spatial diversity and capacity gains, have received a lot of attention in recent years [10]. MIMO-OFDM offers a low-complexity means of achieving channel capacity in a frequency-selective MIMO channel [24]. Pilot-based CFO estimation for MIMO-OFDM has been addressed only very recently [19], [27].

While many blind CFO estimation algorithms have been proposed for single-user OFDM, few can be applied to multiuser multicarrier transmissions. A CP-based approach and a null-subcarrier-based method were developed in [28] and [2], respectively. These algorithms assume that different users have been separated using bandpass filters, which is rather unrealistic unless the frequency offsets for all users are very small.

In this paper, we derive a low-complexity blind CFO estimator based on the optimization of a kurtosis-type cost function. We demonstrate that it outperforms existing blind CFO estimators. In Section II, we consider blind CFO estimation in single-input single-output (SISO) OFDM. We derive the identifiability conditions and analyze the mean-square error (MSE) performance of this new CFO estimator. Criteria similar to kurtosis have been advocated for blind CFO estimation only for SISO-OFDM systems in [6] and [15]. We relate and comment on their differences and similarities with this paper. In Section III, we pursue blind CFO estimation for MIMO-OFDM. The effects of multiple transmit and receive antennas on CFO estimation are investigated. The problem of blind CFO retrieval in a multiuser OFDM-based uplink transmission is addressed in Section IV. We show that the kurtosis-based estimator is able to retrieve CFOs of all users without prior user separation. We also develop frequency-hopping schemes that considerably mitigate the effects of channel nulls and multiuser interference (MUI). Finally, we present our conclusions in Section V.

Notation: Upper- and lower-case bold symbols will be used to denote matrices and column vectors, respectively; $(\cdot)^*$ will denote conjugation; $(\cdot)^{\mathcal{H}}$ Hermitian transpose; $(\cdot)^T$ transpose; $[\mathbf{F}]_{mn} = (N)^{-1/2} \exp(-j2\pi mn/N)$ is the N-point fast Fourier transform (FFT) matrix; $\mathbf{I}_N$ denotes the $N \times N$ identity matrix; $\mathbf{D}^{(M)}(\mathbf{A})$ is a block diagonal matrix with M diagonal blocks, each of which is the matrix $\mathbf{A}$.

Y. Yao was with the Department of Electrical and Computer Engineering, University of Minnesota, Minneapolis, MN 55455 USA. He is now with the Department of Electrical and Computer Engineering, University of Illinois, Chicago, IL 60607 USA (e-mail: yyao@ece.uic.edu).

G. B. Giannakis is with the Department of Electrical and Computer Engineering, University of Minnesota, Minneapolis, MN 55455 USA (e-mail: georgios@ece.umn.edu).

II. SISO-OFDM Systems

A. Input–Output Matrix-Vector Model

Consider OFDM transmissions of block length N, with CP no less than the channel order. After removing the CP, the ith $N \times 1$ received block (OFDM symbol) can be written as

$$\boldsymbol{r}(i) = e^{j\frac{2\pi}{N}i(N+L)\epsilon}\mathbf{D}_N(\epsilon)\mathbf{H}\mathbf{F}^{\mathcal{H}}\boldsymbol{s}(i) + \boldsymbol{w}(i) \qquad (1)$$

where $\mathbf{D}_N(\epsilon) := \text{diag}[1, \exp(j2\pi\epsilon/N), \ldots, \exp(j2\pi(N-1)\epsilon/N)]$, ϵ is the frequency offset, $\boldsymbol{s}(i)$ is the ith block of frequency-domain symbols, $\boldsymbol{w}(i) \sim \mathcal{CN}(\mathbf{0}, \sigma_w^2\mathbf{I}_N)$ represents the channel noise, and $[\mathbf{H}]_{mn} = h((m-n) \bmod N)$ is the channel matrix whose elements are the discrete-time channel impulse response samples $\{h(n)\}_{n=0}^L$. We will assume that the entries of $\boldsymbol{s}(i)$ are independent and circularly symmetric complex random variables. Because the channel matrix $\mathbf{H}$ is circulant, it can be diagonalized by FFT matrices, i.e., $\mathbf{F}\mathbf{H}\mathbf{F}^{\mathcal{H}} = \mathbf{D}_H$, where $\mathbf{D}_H$ is a diagonal matrix whose $(k+1)$st diagonal element is $H(k) := \sum_{l=0}^L h(l)e^{-j2\pi kl/N}$. We thus obtain

$$\boldsymbol{r}(i) = e^{j\frac{2\pi}{N}i(N+L)\epsilon}\mathbf{D}_N(\epsilon)\mathbf{F}^{\mathcal{H}}\mathbf{D}_H\boldsymbol{s}(i) + \boldsymbol{w}(i). \qquad (2)$$

When there is no frequency offset, $\mathbf{D}_N(\epsilon = 0) = \mathbf{I}_N$. Performing FFT on $\boldsymbol{r}(i)$, we then have

$$\boldsymbol{x}(i) := \mathbf{F}\boldsymbol{r}(i) = \mathbf{D}_H\boldsymbol{s}(i) + \mathbf{F}\boldsymbol{w}(i) \qquad (3)$$

confirming that in the absence of CFO, a single-tap equalizer can be used to estimate the symbols in $\boldsymbol{s}(i)$. Now consider the case where $\epsilon \neq 0$. We will assume that the frequency offset is less than half of the subcarrier spacing. For more general cases, the proposed algorithm can be combined with null-subcarrier-based algorithms to extend the acquisition range, or, we may use separate algorithms (e.g., those in [21] and [25]) to estimate the integer part of the offset. When $\epsilon \neq 0$, the FFT output block is

$$\boldsymbol{x}(i) = e^{j\frac{2\pi}{N}i(N+L)\epsilon}\mathbf{F}\mathbf{D}_N(\epsilon)\mathbf{F}^{\mathcal{H}}\mathbf{D}_H\boldsymbol{s}(i) + \mathbf{F}\boldsymbol{w}(i). \qquad (4)$$

Matrix $\mathbf{F}\mathbf{D}_N(\epsilon)\mathbf{F}^{\mathcal{H}}$ is not diagonal, unless $\epsilon = 0$. Hence, the presence of CFO destroys the orthogonality among subcarriers and introduces intercarrier interference (ICI).

B. Kurtosis-Type Cost Function

Let $\hat{\epsilon}$ denote a candidate estimate of the CFO ϵ. Using $\mathbf{D}_N(-\hat{\epsilon})$ to compensate the CFO, and Fourier transforming, we obtain [c.f. (2)]

$$\begin{aligned} \boldsymbol{y}(i) &:= \mathbf{F}\mathbf{D}_N(-\hat{\epsilon})\boldsymbol{r}(i) \\ &= e^{j\frac{2\pi}{N}i(N+L)\epsilon}\mathbf{F}\mathbf{D}_N(\tilde{\epsilon})\mathbf{F}^{\mathcal{H}}\mathbf{D}_H\boldsymbol{s}(i) + \boldsymbol{v}(i) \end{aligned} \qquad (5)$$

where $\tilde{\epsilon} := \epsilon - \hat{\epsilon}$, and $\boldsymbol{v}(i) := \mathbf{F}\mathbf{D}_N(-\hat{\epsilon})\boldsymbol{w}(i) \sim \mathcal{CN}(\mathbf{0}, \sigma_w^2\mathbf{I}_N)$. If $\tilde{\epsilon} = 0$, the noise-free entries of $\boldsymbol{y}(i)$ will equal (within a scale) the source symbols; otherwise, they will be linear combinations of the source symbols. In [9], Donoho shows that a linear combination of independent random variables is closer to Gaussian than the original variables, unless these random variables are Gaussian or the combination is trivial (only one nonzero weight). Since symbols transmitted on different subcarriers are independent and non-Gaussian, the distribution of $\boldsymbol{y}(i)$ is more non-Gaussian when $\tilde{\epsilon} = 0$ than when $\tilde{\epsilon} \neq 0$. This is the key idea behind our blind CFO estimator.

Functions that can be used to measure non-Gaussianity include kurtosis, Fisher's information, and Kullback–Leibler divergence metrics. The normalized kurtosis [26]

$$\text{kurtosis} = \frac{E\left[|y|^4\right] - 2\left(E\left[|y|^2\right]\right)^2 - \left|E[y^2]\right|^2}{\left(E\left[|y|^2\right]\right)^2} \qquad (6)$$

will be used in this paper, for its simplicity and because it leads to a low-complexity closed-form blind CFO estimator. Under the assumption of circularly symmetric complex source symbols, (6) suggests the following objective function to be used in practice:

$$J(\tilde{\epsilon}) = \frac{\sum_{i=0}^{M-1}\sum_{n=0}^{N-1}\frac{|y_n(i)|^4}{M}}{\left(\sum_{i=0}^{M-1}\sum_{n=0}^{N-1}\frac{|y_n(i)|^2}{M}\right)^2} \qquad (7)$$

where $y_n(i)$ is the $(n+1)$st entry of $\boldsymbol{y}(i)$, and M is the number of blocks used in the estimation. To see whether $\tilde{\epsilon} = 0$ is indeed an extreme point of $J(\tilde{\epsilon})$, we examine the behavior of $J(\tilde{\epsilon})$. For M sufficiently large, we can show that (details can be found in Appendix I)

$$J(\tilde{\epsilon}) \cong A \cdot g(\mathbf{H}, \kappa_s)\cos(2\pi\tilde{\epsilon}) + B \qquad (8)$$

where B and $A := 2\sigma_s^4/(\sigma_s^2\sum_{n=0}^{N-1}|H_n|^2 + \sigma_w^2)^2$ are constants independent of $\tilde{\epsilon}$, and

$$g(\mathbf{H}, \kappa_s) = \frac{1}{N^2}\sum_{n=0}^{N-1}\left[\frac{\kappa_s}{6}(N^2-1)|H_n|^4 - \sum_{m \neq n}\frac{|H_mH_n|^2}{\sin^2\frac{(m-n)\pi}{N}}\right] \qquad (9)$$

with $\kappa_s := E[|s_n(i)|^4]/(E[|s_n(i)|^2])^2$. When $g(\mathbf{H}, \kappa_s) > 0$, it follows readily from (8) that $\tilde{\epsilon} = 0$ is a unique global maximum of J. Likewise, when $g < 0$, $\tilde{\epsilon} = 0$ is a unique global minimum.

If the channel order $L \ll N$, we have $|H_m|^2 \cong |H_n|^2$ for neighboring subcarriers m and n, which allows us to write

$$\frac{6}{\kappa_s(N^2-1)}\sum_{m \neq n}\frac{|H_m|^2}{|H_n|^2\sin^2\frac{(m-n)\pi}{N}} > \frac{12}{\kappa_sN^2\sin^2\frac{\pi}{N}} > \frac{12}{\pi^2\kappa_s}. \qquad (10)$$

For most constellations, e.g., quaternary phase-shift keying (QPSK), or square 16-quadrature amplitude modulation (QAM), we have that $12/(\pi^2\kappa_s) > 1$, which implies that $\tilde{\epsilon} = 0$ corresponds to a global minimum of J.

For more general cases, when the symbols (e.g., after precoding) are approximately Gaussian, super-Gaussian ($\kappa_s > 2$), or when the channel order is large, the behavior of $g(\mathbf{H}, \kappa_s)$ in (9) is less clear. To gain more insight, we rewrite (9) as follows:

$$\begin{aligned} g(\mathbf{H}, \kappa_s) &= \frac{1}{N^2}\sum_{m=0}^{N-1}\left[\sum_{n=m+1}^{N-1}\frac{\left(|H_m|^2 - |H_n|^2\right)^2}{\sin^2\frac{(m-n)\pi}{N}}\right. \\ &\quad \left. - \sum_{n=m+1}^{N-1}\frac{|H_m|^4 + |H_n|^4}{\sin^2\frac{(m-n)\pi}{N}} + \frac{\kappa_s}{6}(N^2-1)|H_m|^4\right] \\ &= \frac{1}{N^2}\sum_{m=0}^{N-1}\left\{\sum_{n=m+1}^{N-1}\frac{\left(|H_m|^2 - |H_n|^2\right)^2}{\sin^2\frac{(m-n)\pi}{N}} + |H_m|^4\right. \\ &\quad \left. \times\left[\frac{\kappa_s}{6}(N^2-1) - \sum_{n=1}^{N-1}\frac{1}{\sin^2\frac{n\pi}{N}}\right]\right\}. \end{aligned} \qquad (11)$$

Since $\sum_{n=1}^{N-1} \cot^2(n\pi/N) = (N-1)(N-2)/3$ [3], we have

$$g(\mathbf{H}, \kappa_s) = \frac{1}{N^2} \sum_{m=0}^{N-1} \left[\sum_{n=m+1}^{N-1} \frac{(|H_m|^2 - |H_n|^2)^2}{\sin^2 \frac{(m-n)\pi}{N}} + \frac{1}{6}|H_m|^4(N^2-1)(\kappa_s - 2) \right]. \quad (12)$$

Equation (12) reveals that for super-Gaussian symbol constellations, we always have $g(\mathbf{H}, \kappa_s) > 0$. When transmitting sub-Gaussian symbols, however, we will have $g(\mathbf{H}, \kappa_s) < 0$, if the channel gains do not change rapidly from subcarrier to subcarrier, which corresponds to orders $L \ll N$.

An interesting special case occurs when the symbols are Gaussian. It is well known that for a blind source-separation problem to be solvable, at most one source (here, symbol) can be Gaussian [5]. However, (12) suggests that blind CFO estimation is possible even when all sources are Gaussian, as long as the channel is frequency selective. In this case, we no longer rely on the source non-Gaussianity to retrieve the CFO; but instead, we exploit the power difference between pairs of subcarriers.

C. Low-Complexity Blind CFO Estimator

As discussed previously, a CFO estimate can be obtained by minimizing the function $J(\hat{\epsilon})$. While this can be performed using line search, the regularity of $J(\hat{\epsilon})$ as suggested by (8) makes it possible for us to design estimators with lower complexity. For example, we may use a steepest-descent approach to update $\hat{\epsilon}$ iteratively, or use stochastic gradient-descent alternatives to develop symbol-by-symbol adaptive algorithms. Surprisingly, a closed-form solution is possible using curve fitting. We can evaluate $J(\hat{\epsilon})$ on several points, and then try to find the values of $A \cdot g(\mathbf{H}, \kappa_s)$, B, and ϵ that satisfy (8). For example, if we choose to evaluate $J(x)$ at $x = -1/4, 0, 1/4$, it is easy to see from (8) that an estimate $\hat{\epsilon}$ can be obtained as follows:

$$\hat{\epsilon} = \begin{cases} \frac{1}{2\pi}\sin^{-1}(b), & \text{if } a \geq 0 \\ \frac{1}{2} - \frac{1}{2\pi}\sin^{-1}(b), & \text{if } a < 0 \text{ and } b \geq 0 \\ -\frac{1}{2} - \frac{1}{2\pi}\sin^{-1}(b), & \text{if } a < 0 \text{ and } b \leq 0 \end{cases} \quad (13)$$

where $a := (J(1/4) + J(-1/4))/2 - J(0)$, and $b := (J(-1/4) - J(1/4))/2$. Compared with exhaustive line search, this algorithm has a much lower complexity. Simulations verify that it achieves almost identical performance to that of the more expensive line search.

D. Relation With [6] and [15]

In [15], Luise *et al.* introduced a low-complexity blind CFO estimation algorithm (which we will call LMR). They recognized the duality between CFO estimation in OFDM and timing recovery in a single-carrier system, and proposed a modified version of [22]. Although simulations showed excellent performance, no analytical justification was given. In the LMR scheme, each received OFDM symbol $\boldsymbol{r}(i)$ in (2) with entries $r_n(i)$ is first oversampled in the frequency domain by a factor

N_s to obtain a sequence $\{y'_k\}_{k=0}^{NN_s-1}$, where (dropping i for brevity)

$$y'_k = \frac{1}{\sqrt{NN_s}} \sum_{n=0}^{N-1} r_n e^{-j\frac{2\pi}{NN_s}kn}. \quad (14)$$

A CFO estimate is then obtained as $\hat{\epsilon} = -\arg(-J_{\text{LMR}})/(2\pi)$, where $J_{\text{LMR}} = \sum_{k=0}^{NN_s-1} |y'_k|^4 e^{-j2\pi k/N_s}$. While the absolute value and third-order powers of y'_k can also be used in J_{LMR}, we will focus on the fourth-order powers, since they provide the best performance [15].

Define $y''_k(n_s) := y_{n'_s+kN_s}$, where $n_s = 0, 1, \ldots, N_s - 1$ and $k = 0, 1, \ldots, N - 1$. Then

$$y''_k(n_s) = \frac{1}{\sqrt{NN_s}} \sum_{n=0}^{N-1} r_n e^{-j\frac{2\pi}{N}kn - j\frac{2\pi}{N}\frac{n_s}{N_s}n}. \quad (15)$$

Recall that in our scheme, we have [c.f. (5)]

$$y_k(\hat{\epsilon}) = \frac{1}{\sqrt{N}} \sum_{n=0}^{N-1} r_n e^{-j\frac{2\pi}{N}kn - j\frac{2\pi}{N}n\hat{\epsilon}} \quad (16)$$

With $\hat{\epsilon} := n_s/N_s$, it follows from (15) and (16) that $N_s^2 \sum_{k=0}^{N-1} |y''_k(n_s)|^4 = \sum_{k=0}^{N-1} |y_k(n_s/N_s)|^4 = J_4(n_s/N_s)$, where $J_4(n_s/N_s)$ is the numerator of our cost function $J(\hat{\epsilon} = n_s/N_s)$. Since the denominator of $J(\hat{\epsilon})$ does not depend on $\hat{\epsilon}$ in SISO-OFDM, we have for $N_s \geq 4$ that

$$J_{\text{LMR}} = \sum_{k=0}^{NN_s-1} |y'_k|^4 e^{-j2\pi\frac{k}{N_s}} = \frac{1}{N_s^2} \sum_{n_s=0}^{N_s-1} J_N\left(\frac{n_s}{N_s}\right) e^{-j2\pi\frac{n_s}{N_s}}$$
$$\cong C_1 \sum_{n_s=0}^{N_s-1} A \cdot g(\mathbf{H}, \kappa_s) \cos\left(2\pi\epsilon - \frac{2n_s\pi}{N_s}\right) e^{-j2\pi\frac{n_s}{N_s}}$$
$$= C_2 \cdot g(\mathbf{H}, \kappa_s) e^{-j2\pi\epsilon} \quad (17)$$

where C_1 and C_2 are positive constants independent of ϵ. An estimate of the CFO can thus be obtained as $\hat{\epsilon} = -\arg(g(\mathbf{H}, \kappa_s) J_{\text{LMR}})/(2\pi)$.

Defining $I_k(\epsilon) := |\sum_{l=0}^{N-1} e^{j2\pi(k+\epsilon)l/N}|/N$, and based on the observation that $\sum_{k=0}^{N-1} I_k(\epsilon)$ is a unimodal function of ϵ, Chung and Johnson considered the following cost function [6]:

$$J_{\text{CJ}} = \sum_{n=0}^{N-1} E\left[|y_n(i)|^4\right]. \quad (18)$$

They proved that J_{CJ} can uniquely identify the CFO, provided that channel and symbols satisfy certain conditions [6, Th. 1]. Although J_{CJ} is related to the numerator J_4 of our cost function, our closed forms are different (there seems to be an error in [6], as one can verify by considering the special case of Gaussian symbols).

Basically, both [15] and [6] exploited the fact that higher order statistics of the received OFDM symbols contain a spectral line corresponding to the CFO. We, on the other hand, rely on the distance from Gaussianity. Not only does this perspective lead to more insights on the strengths and limitations of this scheme, but also lends itself naturally to multiuser OFDM and MIMO-OFDM generalizations not addressed in [6] and [15]. Furthermore, this perspective reveals possible

ways of improving CFO estimation performance by adopting more sophisticated measures of non-Gaussianity at the cost of increased complexity.

E. Performance Analysis and Simulated Comparisons

While performance analysis based on either asymptotic (in M) or perturbation analysis is straightforward, the resulting MSE expression is highly complicated, because the cost function is itself a fourth-order statistic. Limiting the channel to be frequency nonselective, we obtain a relatively clean closed-form expression, which sheds light to the performance of the kurtosis-based estimator at high signal-to-noise ratios (SNRs). In particular, we have the following lemma.

Lemma 1: If: 1) the channel is frequency nonselective; 2) the symbols are zero-mean, circularly symmetric complex random variables; 3) the number of OFDM blocks M is large; and 4) the SNR is high; then the MSE of the CFO estimator is approximately

$$
E[\tilde{\epsilon}^2] \cong \frac{3\sigma_w^2}{2\pi^2 MN(N^2-1)^2(2-\kappa_s)^2\sigma_s^2|H|^2}
$$
$$
\times \left[(\rho_s - 9\kappa_s + 12)(N^4 - 5N^3 + 5N^2 + 5N - 6) \right.
$$
$$
\left. +(10\kappa_s - 12)(N^4 - N^2)\right] \tag{19}
$$

where $\rho_s := E[|s|^6]/\sigma_s^6$. If N is large, we can further simplify (19) to

$$
E\left[\tilde{\epsilon}^2\right] \cong \frac{3(\rho_s + \kappa_s)\sigma_w^2}{2\pi^2 MN(2-\kappa_s)^2|H|^2\sigma_s^2}. \tag{20}
$$

Equation (20) reveals that the MSE of the CFO estimator is inversely proportional to the SNR, the OFDM block size N, and the number of blocks M. We also verify that the performance of the blind CFO estimator deteriorates when the symbols' distribution gets close to being Gaussian.

Remark 1: It would be interesting to compare the MSE performance of the proposed CFO estimator with theoretical bounds on blind CFO estimation. Because of the existence of nuisance parameters, namely, the channel coefficients and the source symbols, the bounds available are either the conditional Cramér–Rao bound (CRB) conditioned on channel and source symbols, or the modified CRB (a much looser bound). It was shown in [7] that both the conditional CRB and the modified CRB are equal to infinity when there are no null subcarriers. Since our approach does not rely on null subcarriers, these bounds are not good performance indicators of our algorithm.

We simulate an OFDM transmission over a frequency-selective fading channel. The channel has five independent Rayleigh-fading taps with exponentially decaying powers; in particular, we set $E[|h(l)|^2] = e^{-l/3}/\sum_{l=0}^{4} e^{-l/3}$, $l = 0, \ldots, 4$. We assume that the channel fading is slow enough so that the channel does not change much while CFO estimation is performed. The size of the OFDM block and the length of the CP are 128 and 4, respectively. In each OFDM block, 128 randomly drawn QPSK symbols are transmitted.[1] In Fig. 1, we plot the performance of the kurtosis-based exhaustive search algorithm, the kurtosis-based curve-fitting algorithm (13), the original CP-based algorithm of [29], and the CS-based

---

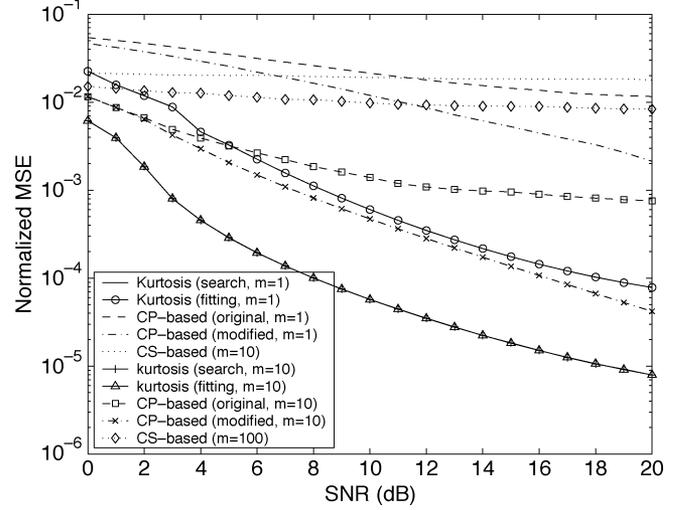[1]This setting will be used throughout this paper unless noted otherwise.

Fig. 1. Performance of different blind CFO estimators in a SISO-OFDM system.

algorithm of [4]. For comparison, we also plot the performance of the modified CP-based algorithm in [16], using a sufficiently long CP of length five. For each algorithm, we perform the simulation using two different sample sizes: $M = 1$, 10 OFDM blocks for kurtosis-based and CP-based algorithms; and $M = 10$, 100 blocks for the CS-based algorithm. We observe that the kurtosis-based algorithms markedly outperform all other algorithms. Interestingly, the low-complexity curve-fitting algorithm performs as well as the exhaustive search algorithm, which also confirms the validity of (8). Among the two CP-based methods, the modified CP-based algorithm outperforms the original algorithm, especially at high SNR. Since the modified CP-based method requires knowledge of the channel order, and a longer than necessary CP, we will use only the original CP-based algorithm as a benchmark in the ensuing simulations. The CS-based algorithm performs much worse than other algorithms, and will not be simulated further.

The bit-error rate (BER) performance of a SISO-OFDM system using the kurtosis-based curve-fitting algorithm to retrieve and compensate for the CFO based on $M = 1$ block is given in Fig. 2. For comparison, we also plot the BER performance of the same system with perfect CFO compensation, with no CFO compensation, and with CP-based CFO estimation and compensation based on $M = 1$ blocks. As expected, without CFO compensation, the system performance suffers serious degradation because of ICI. While the CP-based estimator exhibits a floor in the BER curve at high SNR, the kurtosis-based CFO estimator using (just) one OFDM block achieves almost optimal BER performance.

Remark 2: In order to isolate the ICI effects on BER performance, we have assumed that the channel has been perfectly estimated in our simulation. In practice, the effects of channel-estimation errors and aggregate phase shift across blocks due to the residual CFO must be taken into account. For methods mitigating these effects, we refer the readers to [18] and [30].

In Fig. 3, we compare the MSE of the CFO estimate obtained using Monte-Carlo simulation with the approximation given by *Lemma 1*. A frequency-nonselective channel is assumed. The
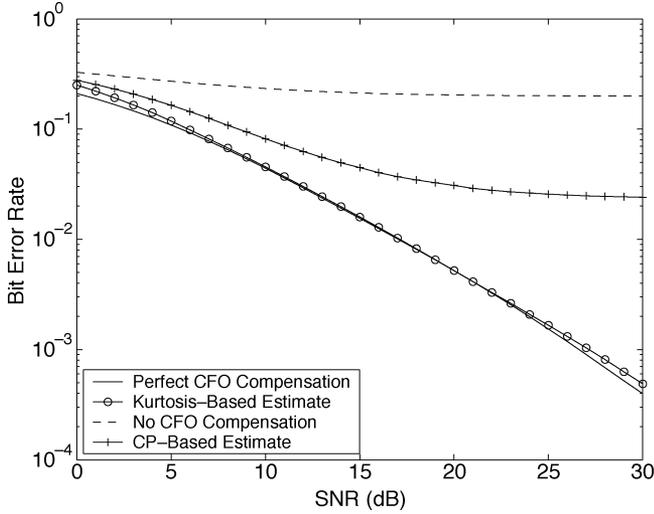
Fig. 2. BER performance of blind CFO estimator in a SISO-OFDM system.

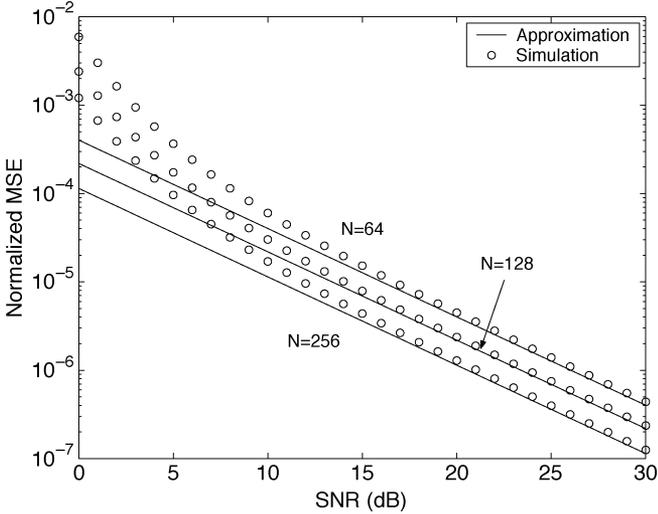Fig. 4. Performance of kurtosis-type CFO estimator with Gaussian-distributed symbols.

Fig. 3. MSE performance of kurtosis-based estimator: Simulation versus approximation.

number of OFDM blocks used is $M = 10$, and three different OFDM block sizes ($N = 64, 128, 256$) are simulated. We observe that the analytical results fit the numerical results quite well at medium-high SNR values.

Blind CFO estimation with Gaussian symbols is very interesting because of the difficulty in separating blindly multiple Gaussian sources, and Gaussian codes are known to achieve Shannon capacity [8]. The performance of the proposed blind CFO estimator when the symbol distribution is Gaussian is studied in Fig. 4. We simulate two extreme cases: when the channel is frequency-flat, and when different subcarriers experience independent fadings. We verify that, as predicted by our analysis, the proposed CFO estimator fails when the channel is flat-fading, while in a frequency-selective channel, it is able to retrieve the CFO information even though the transmitted symbols are Gaussian.
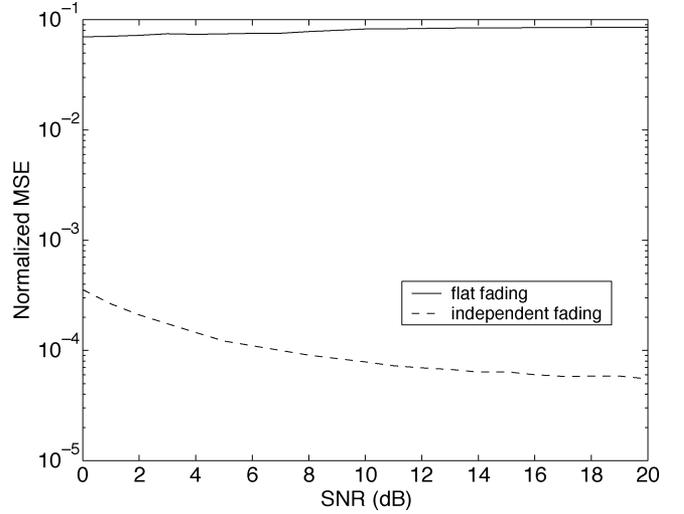
III. MIMO-OFDM SYSTEMS

In this section, we will apply the kurtosis-based CFO estimator to MIMO-OFDM transmissions. We assume that there are M_T transmit antennas and M_R receive antennas. Theoretically, each transmit–receive antenna pair may have a different CFO. In practice, however, the difference among these CFOs is usually negligible, because: 1) even if collocated antennas do not share a radio frequency (RF) oscillator, achieving frequency synchronization among collocated oscillators is relatively easy; and 2) in a number of applications, the Doppler shifts between all transmit–receive antenna pairs are approximately the same. For this reason, similar to [18], [27] and [30], we focus on MIMO-OFDM systems experiencing a single common CFO among transmit–receive antennas. On denoting
$$\boldsymbol{r}(i) := [r_{1,0}(i) \cdots r_{1,N-1}(i) \cdots r_{M_R,0}(i) \cdots r_{M_R,N-1}(i)]^T,$$
$$\boldsymbol{s}(i) := [s_{1,0}(i) \cdots s_{1,N-1}(i) \cdots s_{M_T,0}(i) \cdots s_{M_T,N-1}(i)]^T,$$
and $\boldsymbol{w}(i) := [w_{1,0}(i) \cdots w_{1,N-1}(i) \cdots w_{M_R,0}(i) \cdots w_{M_R,N-1}(i)]^T$, the output at the receiver after CP removal can be written as

$$\boldsymbol{r}(i) = e^{j\frac{2\pi}{N}i(N+L)\epsilon} \mathbf{D}^{(M_R)}\left(\mathbf{D}_N(\epsilon)\right)\mathbf{H}\mathbf{D}^{(M_T)}(\mathbf{F}^{\mathcal{H}})\boldsymbol{s}(i) + \boldsymbol{w}(i) \tag{21}$$

where the channel matrix $\mathbf{H}$ consists of $M_R \times M_T$ subblocks

$$\mathbf{H} = \begin{bmatrix} \mathbf{H}_{1,1} & \cdots & \mathbf{H}_{1,M_T} \\ \vdots & \ddots & \vdots \\ \mathbf{H}_{M_R,1} & \cdots & \mathbf{H}_{M_R,M_T} \end{bmatrix} \tag{22}$$

and the subblock $\mathbf{H}_{m,n}$ is an $N \times N$ circulant matrix representing the channel between the nth transmit and the mth receive antenna; i.e., its first column is $[h_{m,n}(L), \ldots, h_{m,n}(0), 0, \ldots, 0]^T$. Using the property of the circulant matrices

$$\boldsymbol{x}(i) := \mathbf{D}^{(M_R)}(\mathbf{F})\boldsymbol{r}(i)$$
$$= e^{j\frac{2\pi}{N}i(N+L)\epsilon} \mathbf{D}^{(M_R)}\left(\mathbf{F}\mathbf{D}_N(\epsilon)\mathbf{F}^{\mathcal{H}}\right)\boldsymbol{\Lambda}\boldsymbol{s}(i)$$
$$+ \mathbf{D}^{(M_R)}(\mathbf{F})\boldsymbol{w}(i) \tag{23}$$

Fig. 5.   Performance of kurtosis-based CFO estimator in MIMO-OFDM.
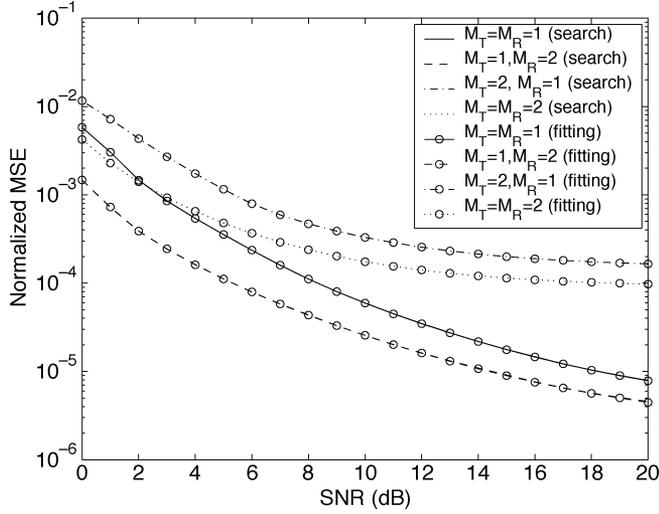

Fig. 6.   BER performance of blind CFO estimator in MIMO-OFDM.

where

$$\mathbf{\Lambda} := \begin{bmatrix} \mathbf{\Lambda}_{1,1} & \dots & \mathbf{\Lambda}_{1,M_T} \\ \vdots & \ddots & \vdots \\ \mathbf{\Lambda}_{M_R,1} & \dots & \mathbf{\Lambda}_{M_R,M_T} \end{bmatrix}. \tag{24}$$

The subblocks of $\mathbf{\Lambda}$ are diagonal matrices: $\mathbf{\Lambda}_{m,n} := \mathrm{diag}(\lambda_{m,n}(0), \dots, \lambda_{m,n}(N - 1))$, and $\lambda_{m,n}(k) := \sum_{l=0}^{L} h_{m,n}(l) \exp(-j2\pi kl/N)$. On denoting $\boldsymbol{x}_r(i) := [x_{r,0}(i) \dots x_{r,N-1}(i)]^T$, $\boldsymbol{w}_r(i) := [w_{r,0}(i) \dots w_{r,N-1}(i)]^T$, and $\boldsymbol{s}_t(i) := [s_{t,0}(i) \dots s_{t,N-1}(i)]^T$, we have

$$\boldsymbol{x}_r(i) = e^{j\frac{2\pi}{N}i(N+L)\epsilon}\mathbf{F}\mathbf{D}_N(\epsilon)\mathbf{F}^{\mathcal{H}}\sum_{t=1}^{M_T}\mathbf{\Lambda}_{r,t}\boldsymbol{s}_t(i) + \mathbf{F}\boldsymbol{w}_r(i). \tag{25}$$

We can verify that for $\epsilon \in [-0.5, 0.5]$, the ICI disappears only if $\epsilon = 0$. Similar to SISO-OFDM, we introduce the following kurtosis-type cost function for MIMO-OFDM:

$$J(\tilde{\epsilon}) = \frac{\sum_{i=0}^{M-1}\sum_{r=1}^{M_R}\sum_{n=0}^{N-1}|y_{r,n}(i)|^4}{\left(\sum_{i=0}^{M-1}\sum_{r=1}^{M_R}\sum_{n=0}^{N-1}|y_{r,n}(i)|^2\right)^2} \tag{26}$$

where
$\boldsymbol{y}(i) := [y_{1,0}(i) \dots y_{1,N-1}(i) \dots y_{M_T,0}(i) \dots y_{M_T,N-1}(i)]^T$ is obtained as follows:

$$\boldsymbol{y}(i) = \mathbf{D}^{(M_R)}\left(\mathbf{F}\mathbf{D}_N(-\hat{\epsilon})\right)\boldsymbol{r}(i). \tag{27}$$

Fig. 5 shows the performance of the kurtosis-based CFO estimator in MIMO-OFDM systems with different numbers of transmit and receive antennas, based on $M = 10$ blocks. Channels between different antenna pairs are independent. As expected, multiple receive antennas improve CFO estimation performance, thanks to receive diversity gain. When there are multiple transmit antennas, the MSE performance of the CFO estimator exhibits an error floor, because the coupling between different transmit antennas brings the symbol distribution closer to Gaussian. Hence, we must exercise caution in
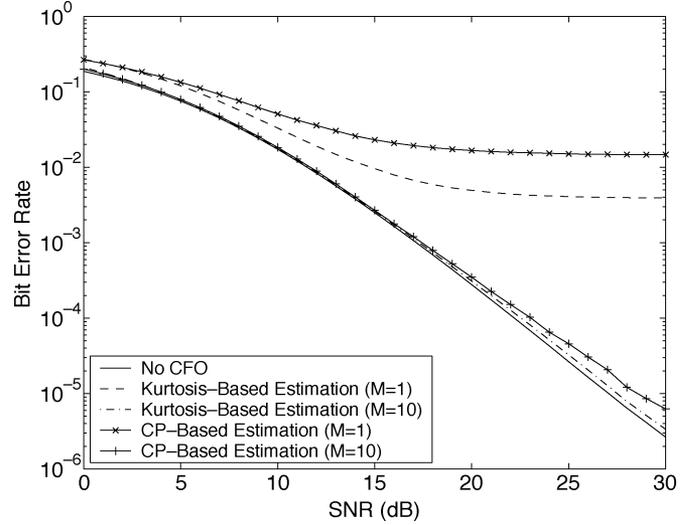
applying this method to systems with many (e.g., $M_T > 10$) transmit antennas and space–time coding.[2] We also compare the performance of the line search with the curve-fitting algorithm. We observe that they have almost identical performance, suggesting that the low-complexity curve-fitting algorithm can also be applied to MIMO systems.

In MIMO systems, space–time codes are often used to improve rate and/or error performance. The kurtosis-based CFO estimator is applicable to MIMO-OFDM systems *regardless* of the underlying space–time code that may be employed. We simulate the BER performance of a MIMO-OFDM system ($M_T = 2$, $M_R = 1$) when there is no CFO, and when $M = 1$ and $M = 10$ OFDM blocks are used for CFO estimation, respectively. The kurtosis-based curve-fitting algorithm is used for CFO estimation, and Alamouti's code [1] is employed to effect diversity gains. From Fig. 6, we observe that, unlike the SISO case, significant BER performance loss is incurred if only one OFDM block is used for CFO estimation. However, we also observe that when $M = 10$, the BER performance loss caused by imperfect CFO estimation is negligible. So, although kurtosis-based CFO estimation exhibits a MSE floor when there are multiple transmit antennas, this MSE floor does not translate to a BER floor. For comparison, we have also plotted the performance of CP-based estimator ($M = 1$ and $M = 10$). Again, the kurtosis-based CFO estimator outperforms the CP-based estimator.

IV. MULTIUSER UPLINK OFDM

Blind CFO estimation in multiuser uplink OFDM transmissions is a challenging problem, because different users experience different channel fadings and may have different CFOs. The CP-based method of [28] is sensitive to MUI, because different users' CPs overlap. When using the null-subcarrier-based method of [2], large guard bands are needed to alleviate the energy leakage from neighboring users. In this section, we extend

---

[2]Systems using transmit beamforming do not face this limitation, because the same data symbols are transmitted by every antenna element.
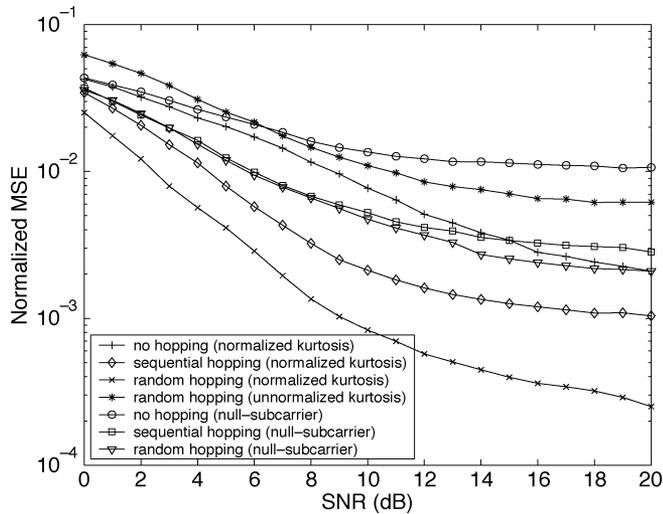
Fig. 7. Performance of blind CFO estimator in a multiuser uplink OFDM system.

Fig. 8. Performance of kurtosis-based estimators with variable guard-band sizes.

the kurtosis-based method to the multiuser case. We will demonstrate that it works even when the guard bands are relatively small.

Suppose there are K users, each transmitting on a set of N_a contiguous subcarriers. Between two neighboring users, there are N_g null subcarriers serving as guard bands. Assuming that user k occupies the band from subcarrier a_k to subcarrier b_k, the kurtosis-based cost function for estimating user k's CFO can be written as

$$J_k(\tilde{\epsilon}) = \frac{\sum_{i=0}^{M-1} \sum_{n=a_k}^{b_k} \frac{|y_n(i)|^4}{M}}{\left(\sum_{i=0}^{M-1} \sum_{n=a_k}^{b_k} \frac{|y_n(i)|^2}{M} \right)^2}. \qquad (28)$$

Since one user occupies only a portion of the frequency band, he/she is more susceptible to the effects of channel nulls. To mitigate this effect, interleaved OFDMA can be used in place of subband-based orthogonal frequency-division multiple access (OFDMA). Interleaved OFDMA, however, is more susceptible to MUI. In [2], frequency hopping was suggested to achieve channel-independent synchronization. In particular, during the pth block, the kth user is assigned the subcarriers $(kN_t + i_p, kN_t + 1 + i_p, \ldots, kN_t + N_a - 1 + i_p)$, where $N_t := N_a + N_g$, and i_p is the frequency-hopping index. While this scheme, which we will henceforth call sequential hopping, mitigates the effects of possible channel nulls, it does not address the near–far effect users may experience in a multiple-access scenario. This is particularly relevant in uplink transmissions, because different users may have different powers, different frequency offsets, and may experience different channel fading. To deal with this problem, our idea is to combine frequency hopping with user permutation. Specifically, we divide the entire frequency band into K equispaced frequency subbands, each consisting of N_a subcarriers. During each block, each user will be randomly assigned one of the subbands. In the following, we will demonstrate that this random-hopping scheme makes our CFO estimator more robust to MUI.

In Fig. 7, we test performance of the kurtosis-based estimator using different hopping schemes. There are eight users, each
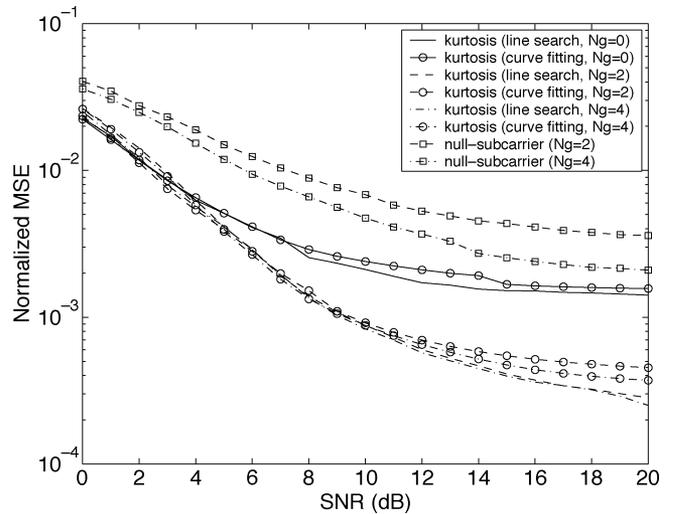
occupying $N_a = 12$ subcarriers with $N_g = 4$ null subcarriers between neighboring users. $M = 16$ OFDM blocks are used for CFO estimation. Since the CP-based algorithm does not work without first separating the users, we will use the null-subcarrier-based method [2] for comparison. We observe that random hopping achieves a large gain over sequential hopping. Both of these two schemes significantly outperform the scheme without hopping. Unlike the single-user case, the denominator of the cost function (28) depends on $\tilde{\epsilon}$. From Fig. 7, we verify that if the cost function contains only the numerator of (28) (which corresponds to "unnormalized kurtosis" similar to those in [6] and [15]), the performance of the blind CFO estimator will degrade significantly. Compared with the null-subcarrier-based algorithm, the kurtosis-based estimator attains a much lower MSE.

To see how our algorithm performs with small guard bands, we simulate the cases when the guard band between two neighboring users consists of zero, two, and four null subcarriers, respectively. For comparison, we again use the null-subcarrier-based algorithm as a benchmark. From Fig. 8, we observe that the kurtosis-based algorithm significantly outperforms the null-subcarrier-based method. When the size of the guard bands is decreased from four to two, performance of the null-subcarrier-based estimator degrades, while the kurtosis-based method suffers only a minor performance loss. When the guard bands are removed, the kurtosis-based estimator suffers considerable performance loss, but still outperforms the null-subcarrier-based algorithm with guard bands. In this figure, we also plot the performance of the low-complexity curve-fitting algorithm, as described by (13), under all three scenarios. Different from the single-user case, where its performance is as good as the more expensive search algorithm, in multiuser transmissions, it performs slightly worse than the search algorithm. Nevertheless, the gaps are relatively small in all three cases, indicating that this low-complexity method has great potential.

The BER performance of the kurtosis-based curve-fitting algorithm in a multiuser OFDM uplink transmission is shown in Fig. 9. For CFO estimation, $M = 10$ OFDM blocks are used.
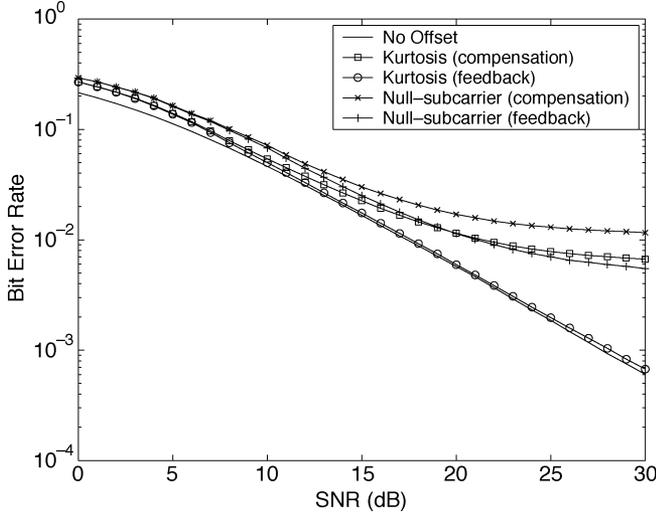
Fig. 9. BER performance of kurtosis-based estimator in a multiuser OFDM system.

Because different users have different CFOs, attempting to compensate one user's CFO at the receiver will cause some other users' CFOs to increase. This will increase the ICI coming from these users. Therefore, CFO compensation at the receiver will not completely eliminate the ICI. We can verify from Fig. 9 that CFO compensation incurs noticeable performance loss at high SNR. On the other hand, by feeding back CFO estimates to users and asking them to adjust their carrier frequencies accordingly at the transmitters, we are able to achieve BER performance very close to that of systems without CFO. For comparison, we also plot the BER performance obtained using the null-subcarrier-based algorithm. Again, we can verify that the kurtosis-based estimator achieves much better performance.

V. CONCLUSIONS

We developed a kurtosis-based blind CFO estimator for OFDM systems. We demonstrated that this novel cost function is able to uniquely identify the CFO within the range of half-subcarrier spacing, while lending itself to very low-complexity algorithms. A closed-form expression for the MSE of the CFO estimate was obtained for frequency-flat channels. We also applied this approach to MIMO-OFDM and multiuser OFDM systems. For MIMO-OFDM, we investigated the effects of multiple transmit and receive antennas on the performance of the CFO estimator. For multiuser OFDM transmissions, we introduced a random-hopping scheme which robustifies the proposed CFO estimator against channel nulls and MUI. We demonstrated that in multiuser OFDM, the kurtosis-based CFO estimator achieves satisfactory performance, even when the size of the guard bands is small.

In our study of MIMO-OFDM CFO estimation, we have assumed that the CFOs for different transmit–receive antenna pairs are approximately the same. Although this assumption is realistic in many scenarios, there are some applications in which different antenna pairs have different CFOs. One example is

the distributed space–time system that has attracted a lot of attention in recent years. Designing blind or even training-based CFO estimators for these systems is a challenging problem, and constitutes an interesting future research topic.[3]

APPENDIX I
DERIVATION OF (8) AND (9)

When M is large, the sample kurtosis approaches its ensemble counterpart

$$J(\tilde{\epsilon}) \cong \frac{\sum_{n=0}^{N-1} E\left[|y_n(i)|^4\right]}{\left(\sum_{n=0}^{N-1} E\left[|y_n(i)|^2\right]\right)^2}. \tag{29}$$

Assuming that the source symbols and noise are zero-mean, circularly symmetric complex random variables, we have (after dropping the block index i for brevity)

$$\sum_{n=0}^{N-1} E\left[|y_n|^4\right] = \sum_{n=0}^{N-1} E\big[|\bar{y}_n|^4 + |v_n|^4 + 2|\bar{y}_n|^2|v_n|^2$$
$$+ 4|v_n|^2 \Re\left(\bar{y}_n^* v_n\right) + 4|\bar{y}_n|^2 \Re\left(\bar{y}_n^* v_n\right)\big]$$
$$= \sum_{n=0}^{N-1} \left(E\left[|\bar{y}_n|^4\right] + E\left[|v_n|^4\right] + 2\sigma_w^2 E\left[|\bar{y}_n|^2\right]\right) \tag{30}$$

where $\bar{y}_n := y_n - v_n$, and in establishing the above equalities, we used the fact that $\bar{y}_n$ is independent of v_n. Since $\sum_{n=0}^{N-1} E[|\bar{y}_n|^2]$ is the total energy of the noise-free received signal, and does not change with $\tilde{\epsilon}$, we have that $\sum_{n=0}^{N-1} E[|y_n|^4] = \sum_{n=0}^{N-1} E[|\bar{y}_n|^4] + C_1$, where C_1 is a constant independent of $\hat{\epsilon}$. Writing the noise-free part of (5) component-wise, we have

$$\bar{y}_n = \frac{1}{N} \sum_{k=0}^{N-1} H_k s_k \sum_{l=0}^{N-1} e^{j\frac{2\pi}{N}(\tilde{\epsilon}+k-n)l}. \tag{31}$$

Therefore, $\sum_{n=0}^{N-1} E[|\bar{y}_n|^4]$ can be written as

$$\sum_{n=0}^{N-1} E\left[|\bar{y}_n|^4\right]$$
$$= \frac{1}{N^4} \sum_{pp'qq'lkl'k'=0}^{N-1} H_k H_l^* H_{k'} H_{l'}^* E\left[s_k s_l^* s_{k'} s_{l'}^*\right]$$
$$\times \sum_{n=0}^{N-1} e^{j\frac{2\pi}{N}\left[(\tilde{\epsilon}-n)(p-p'+q-q')+(pk-p'l+qk'-q'l')\right]}$$
$$:= \frac{1}{N^4} \sum_{l,k,l',k'=0}^{N-1} T_{lkl'k'}. \tag{32}$$

The summands in (32) are nonzero only if $k = l = k' = l'$, $k = l \neq k' = l'$, or $k = l' \neq l = k'$. When $k = l = k' = l'$, we have

$$
\begin{aligned}
T_{kkkk} &= \sum_{n=0}^{N-1} \sum_{p,p',q,q'=0}^{N-1} |H_k|^4 E\left[|s_k|^4\right] e^{j\frac{2\pi}{N}(p-p'+q-q')(\tilde{\epsilon}-n+k)} \\
&= 2N \cos(2\pi\tilde{\epsilon}) \sum_{pp'qq' \in \boldsymbol{\Omega}} |H_k|^4 E\left[|s_k|^4\right] + C_2
\end{aligned}
\tag{33}
$$

where C_2 is a constant independent of $\tilde{\epsilon}$, and $\boldsymbol{\Omega} = \{(p,p',q,q') \mid 0 \leq p,p',q,q' \leq N-1, \ p-p'+q-q' = N\}$. For $p-p'+q-q' = N$, we must have $p-p' > 0$. Given $\rho := p-p'$, there are ρ pairs of (q,q') that satisfy $q-q' = N-\rho$. So

$$
\begin{aligned}
T_{kkkk} &= 2N \cos(2\pi\tilde{\epsilon})|H_k|^4 E\left[|s_k|^4\right] \sum_{\rho=1}^{N-1} \rho(N-\rho) + C_2 \\
&= \frac{1}{3} N^2(N^2-1)\cos(2\pi\tilde{\epsilon})|H_k|^4 E\left[|s_k|^4\right] + C_2.
\end{aligned}
\tag{34}
$$

Similarly, we can obtain that

$$
\begin{aligned}
T_{kkk'k'} &= T_{k'kkk'} \\
&= 2N\cos(2\pi\tilde{\epsilon})|H_k H_{k'}|^2 E\left[|s_k|^2\right] E\left[|s_{k'}|^2\right] \\
&\quad \times \sum_{\rho=1}^{N-1} \rho(N-\rho) e^{\frac{2\pi}{N}\rho(k-k')} + C_3 \\
&= -N^2\cos(2\pi\tilde{\epsilon}) \\
&\quad \times \frac{|H_k H_{k'}|^2 E\left[|s_k|^2\right] E\left[|s_{k'}|^2\right]}{\sin^2\frac{(k-k')\pi}{N}} + C_3
\end{aligned}
\tag{35}
$$

where C_3 is a constant independent of $\tilde{\epsilon}$.

Assuming that source distributions on different subcarriers are identical, and letting $\sigma_s^2 := E[|s_k|^2]$, we have

$$
\begin{aligned}
\sum_{n=0}^{N-1} E\left[|\bar{y}_n|^4\right] &= \frac{1}{N^4} \sum_{k=0}^{N-1} \left[T_{kkkk} + \sum_{k' \neq k}(T_{kkk'k'} + T_{k'kkk'}) \right] \\
&= \frac{2\sigma_s^4 \cos(2\pi\tilde{\epsilon})}{N^2} \sum_{k=0}^{N-1} \left\{ \frac{\kappa_s}{6}(N^2-1)|H_k|^4 \right. \\
&\quad \left. - \sum_{k' \neq k} \frac{|H_k H_{k'}|^2}{\sin^2\frac{(k-k')\pi}{N}} \right\} + C_4
\end{aligned}
\tag{36}
$$

where C_4 is a constant independent of $\tilde{\epsilon}$.

The denominator of (29) can be readily shown to be

$$
\left(\sum_{n=0}^{N-1} E\left[|y_n(i)|^2\right]\right)^2 = \left(\sigma_s^2 \sum_{n=0}^{N-1} |H_n|^2 + \sigma_w^2\right)^2
\tag{37}
$$

which does not depend on $\tilde{\epsilon}$, because it is just the square of the total signal and noise energy (excluding the CP). Note that, while this term may appear to be redundant here, it is needed to compensate for the energy leakage and MUI we will encounter in multiuser OFDM transmissions. Combining (36) and (37) yields (8).

Remark 3: While we have assumed a deterministic channel $\mathbf{H}$ here, it is straightforward to extend our results to fading channels by taking expectation of (8) over channel realizations.

APPENDIX II
PROOF OF *LEMMA 1*

Since in single-user OFDM systems, the denominator in (7) does not depend on $\tilde{\epsilon}$, we will focus on the numerator. Following arguments similar to those used in [2], we can show that, under our assumptions, the MSE of the CFO estimation error can be approximated by

$$
E[\tilde{\epsilon}^2] = E\left\{ \frac{\left|\frac{d\delta J_{s+w}(0)}{d\tilde{\epsilon}}\right|^2}{\left|\frac{d^2 J_s(0)}{d\tilde{\epsilon}^2}\right|^2} \right\}
\tag{38}
$$

where

$$
J_s(\tilde{\epsilon}) := \frac{1}{M} \sum_{i=1}^{M} \sum_{n=0}^{N-1} |\bar{y}_n(i)|^4
\tag{39}
$$

$$
\delta J_{s+w}(\tilde{\epsilon}) := \frac{1}{M} \sum_{i=1}^{M} \sum_{n=0}^{N-1} |y_n(i)|^4 - J_s(\tilde{\epsilon}).
\tag{40}
$$

Since

$$
\begin{aligned}
J_s(\tilde{\epsilon}) &= \frac{|H|^4}{MN^4} \sum_{i=1}^{M} \sum_{n=0}^{N-1} \sum_{\boldsymbol{k},\boldsymbol{l}} s_{l_1}(i)s_{l_2}^*(i)s_{l_3}(i)s_{l_4}^*(i) \\
&\quad \times e^{j\frac{2\pi}{N}[(-\tilde{\epsilon}-n)(k_1-k_2+k_3-k_4)+k_1 l_1-k_2 l_2+k_3 l_3-k_4 l_4]} \\
&= \frac{|H|^4}{MN^3} \sum_{i=1}^{M} \sum_{\boldsymbol{k},\boldsymbol{l}} s_{l_1}(i)s_{l_2}^*(i)s_{l_3}(i)s_{l_4}^*(i) \\
&\quad \times e^{j\frac{2\pi}{N}(k_1 l_1-k_2 l_2+k_3 l_3-k_4 l_4)} \\
&\quad \times \left[1(\boldsymbol{k} \in \Omega^+)e^{-j2\pi\tilde{\epsilon}} + 1(\boldsymbol{k} \in \Omega^-)e^{-j2\pi\tilde{\epsilon}}\right]
\end{aligned}
\tag{41}
$$

where $\boldsymbol{k} := \{k_1, k_2, k_3, k_4\}$, $\boldsymbol{l} := \{l_1, l_2, l_3, l_4\}$, $1(\cdot)$ is the indicator function, and $\Omega^{\pm} := \{\boldsymbol{k} \mid k_1 - k_2 + k_3 - k_4 = \pm N\}$. Taking the second-order derivative, we readily obtain

$$
\begin{aligned}
\frac{d^2 J_s(0)}{d\tilde{\epsilon}^2} &= -\frac{4\pi^2|H|^4}{MN^3} \sum_{i=1}^{M} \sum_{\boldsymbol{k},\boldsymbol{l}} s_{l_1}(i)s_{l_2}^*(i)s_{l_3}(i)s_{l_4}^*(i) \\
&\quad \times e^{j\frac{2\pi}{N}(k_1 l_1-k_2 l_2+k_3 l_3-k_4 l_4)} \times 1(\boldsymbol{k} \in \Omega^+ \cup \Omega^-) \\
&\cong -\frac{4\pi^2|H|^4}{MN^3} \sum_{\boldsymbol{k},\boldsymbol{l}} E\left[s_{l_1}s_{l_2}^*s_{l_3}s_{l_4}^*\right] \\
&\quad \times 1(\boldsymbol{k} \in \Omega^+ \cup \Omega^-) \times e^{j\frac{2\pi}{N}(k_1 l_1-k_2 l_2+k_3 l_3-k_4 l_4)} \\
&= \frac{4\pi^2|H|^4\sigma_s^4}{3N}(N^2-1)(2-\kappa_s).
\end{aligned}
\tag{42}
$$

Now let us examine $\delta J_{s+w}(\tilde{\epsilon})$. Using a first-order approximation, we can show that

$$
\delta J_{s+w}(\tilde{\epsilon}) \cong \frac{4}{M} \sum_{i=1}^{M} \sum_{n=0}^{N-1} |\bar{y}_n(i)|^2 \Re\left(\bar{y}_n(i) v_n^*(i)\right)
$$

$$
= \frac{2|H|^2}{MN^2\sqrt{N}} \sum_{i=1}^{M} \sum_{\boldsymbol{k},\boldsymbol{l}} s_{l_1}(i) s_{l_2}^*(i) e^{-j\frac{2\pi}{N}(k_1 l_1 - k_2 l_2)}
$$

$$
\times \Big\{ H s_{l_3}(i) w_{k_4}^*(i) e^{j\frac{2\pi}{N} k_3 l_3}
$$

$$
\times \left[1(\boldsymbol{k} \in \Omega^+) e^{-j2\pi\tilde{\epsilon}} + (\boldsymbol{k} \in \Omega^-) e^{j2\pi\tilde{\epsilon}} \right]
$$

$$
+ H^* s_{l_3}^*(i) w_{k_4}(i) e^{-j\frac{2\pi}{N} k_3 l_3}
$$

$$
\times \left[1(\boldsymbol{k} \in \Theta^+) e^{-2\pi\tilde{\epsilon}} + 1(\boldsymbol{k} \in \Theta^-) e^{2\pi\tilde{\epsilon}} \right] \Big\}. \quad (43)
$$

Taking the first-order derivative, we have

$$
\frac{d\delta J_{s+w}(0)}{d\tilde{\epsilon}}
$$

$$
\cong \frac{j4\pi|H|^2}{MN^2\sqrt{N}} \sum_{i=1}^{M} \sum_{\boldsymbol{k},\boldsymbol{l}} s_{l_1}(i) s_{l_2}^*(i) e^{j\frac{2\pi}{N}(k_1 l_1 - k_2 l_2)}
$$

$$
\times \Big\{ H s_{l_3}(i) w_{k_4}^*(i) e^{j\frac{2\pi}{N} k_3 l_3} \left[1(\boldsymbol{k} \in \Omega^-) - 1(\boldsymbol{k} \in \Omega^+) \right]
$$

$$
+ H^* s_{l_3}^*(i) w_{k_4}(i) e^{-j\frac{2\pi}{N} k_3 l_3} \left[1(\boldsymbol{k} \in \Theta^-) - 1(\boldsymbol{k} \in \Theta^+) \right] \Big\}. \quad (44)
$$

After some tedious but straightforward algebra, we arrive at

$$
E\left[\left| \frac{d\delta J_{s+w}(0)}{d\tilde{\epsilon}} \right|^2 \right] \cong \frac{8\pi^2 |H|^6 \sigma_w^2}{3MN^3}
$$

$$
\times \Big\{ \left(E[|s|^6 - 9E\left[|s|^4\right] \sigma_s^2 + 12\sigma_s^6) \right)
$$

$$
\times (N^4 - 5N^3 + 5N^2 + 5N - 6)
$$

$$
+ \left(10E\left[|s|^4\right] \sigma_s^2 - 12\sigma_s^6 \right)
$$

$$
\times (N^4 - N^2) \Big\}. \quad (45)
$$

Combining (38), (42), and (45), we obtain *Lemma 1*.

REFERENCES

[1] S. M. Alamouti, "A simple transmit diversity technique for wireless communications," *IEEE J. Sel. Areas Commun.*, vol. 16, pp. 1451–1458, Oct. 1998.

[2] S. Barbarossa, M. Pompili, and G. B. Giannakis, "Channel-independent synchronization of orthogonal frequency-division multiple-access systems," *IEEE J. Sel. Areas Commun.*, vol. 20, pp. 474–486, Feb. 2002.

[3] B. C. Berndt and B. P. Yeap, "Explicit evaluations and reciprocity theorems for finite trigonometric sums," *Adv. Appl. Math.*, vol. 29, no. 3, pp. 358–385, Oct. 2002.

[4] H. Bölcskei, "Blind estimation of symbol timing and carrier frequency offset in wireless OFDM systems," *IEEE Trans. Commun.*, vol. 49, pp. 988–999, Jun. 2001.

[5] J. F. Cardoso, "Blind signal separation: Statistical principles," *Proc. IEEE*, vol. 86, pp. 2009–2025, Oct. 1998.

[6] W. Chung and C. R. Johnson, "Blind carrier frequency offset synchronization for OFDM systems based on higher order statistics," in *Proc. of Conf. Inf. Sci. Syst.*, Princeton, NJ, Mar. 2002, pp. 624–629.

[7] M. Ghogho, A. Swami, and G. B. Giannakis, "Optimized null-subcarrier selection for CFO estimation in OFDM over frequency-selective fading channels," in *Proc. IEEE GLOBECOM*, vol. 1, San Antonio, TX, Nov. 2001, pp. 202–206.

[8] T. M. Cover and J. A. Thomas, *Elements of Information Theory*. New York: Wiley, 1991.

[9] D. Donoho, "On minimum entropy deconvolution," in *Applied Time-Series Analysis II*. New York: Academic, 1981, pp. 569–609.

[10] G. J. Foschini and M. J. Gans, "On limits of wireless communications in a fading environment when using multiple antennas," *Wireless Pers. Commun.*, vol. 6, no. 3, pp. 311–335, Mar. 1998.

[11] M. Ghogho and A. Swami, "Blind frequency-offset estimator for OFDM systems transmitting constant-modulus symbols," *IEEE Commun. Lett.*, vol. 6, pp. 343–345, Aug. 2002.

[12] M.-H. Hsieh and C.-H. Wei, "A low-complexity frame synchronization and frequency offset compensation scheme for OFDM systems over fading channels," *IEEE Trans. Veh. Technol.*, vol. 48, pp. 1596–1609, Sep. 1999.

[13] N. Lashkarian and S. Kiaei, "Class of cyclic-based estimators for frequency-offset estimation of OFDM systems," *IEEE Trans. Commun.*, vol. 48, pp. 2139–2149, Dec. 2000.

[14] H. Liu and U. Tureli, "A high-efficiency carrier estimator for OFDM communications," *IEEE Commun. Lett.*, vol. 2, pp. 104–106, Apr. 1998.

[15] M. Luise, M. Marselli, and R. Reggiannini, "Low-complexity blind carrier frequency recovery for OFDM signals over frequency-selective radio channels," *IEEE Trans. Commun.*, vol. 50, pp. 1182–1188, Jul. 2002.

[16] X. Ma, G. B. Giannakis, and S. Barbarossa, "Non-data aided frequency-offset and channel estimation in OFDM and related block transmissions," in *Proc. Int. Conf. Commun.*, vol. 6, Helsinki, Finland, Jun. 2001, pp. 1866–1870.

[17] X. Ma, C. Tepedelenlioğlu, G. B. Giannakis, and S. Barbarossa, "Non-data-aided carrier offset estimators for OFDM with null subcarriers: Identifiability, algorithms, and performance," *IEEE J. Sel. Areas Commun.*, vol. 19, pp. 2504–2515, Dec. 2001.

[18] X. Ma, M.-K. Oh, G. B. Giannakis, and D.-J. Park, "Hopping pilots for estimation of frequency-offset and multiantenna channels in MIMO-OFDM," *IEEE Trans. Commun.*, vol. 53, pp. 162–172, Jan. 2005.

[19] A. N. Mody and G. L. Stüber, "Synchronization for MIMO OFDM systems," in *Proc. GLOBECOM*, vol. 1, San Antonio, TX, Nov. 2001, pp. 509–513.

[20] P. H. Moose, "A technique for orthogonal frequency-division multiplexing frequency offset correction," *IEEE. Trans. Commun.*, vol. 42, pp. 2908–2914, Oct. 1994.

[21] M. Morelli, A. N. D'Andrea, and U. Mengali, "Frequency ambiguity resolution in OFDM systems," *IEEE Commun. Lett.*, vol. 4, pp. 134–136, Apr. 2000.

[22] M. Oerder and H. Meyr, "Digital filter and square timing recovery," *IEEE Trans. Commun.*, vol. COM-36, pp. 605–612, May 1988.

[23] T. Pollet, M. van Bladel, and M. Moeneclaey, "BER sensitivity of OFDM systems to carrier frequency offset and Wiener phase noise," *IEEE Trans. Commun.*, vol. 43, pp. 191–193, Feb.–Apr. 1995.

[24] G. G. Raleigh and J. M. Cioffi, "Spatio-temporal coding for wireless communication," *IEEE Trans. Commun.*, vol. 46, pp. 357–366, Mar. 1998.

[25] T. M. Schmidl and D. C. Cox, "Robust frequency and timing synchronization for OFDM," *IEEE Trans. Commun.*, vol. 45, pp. 1613–1621, Dec. 1997.

[26] J. K. Tugnait, "Identification and deconvolution of multichannel linear non-Gaussian processes using higher-order statistics and inverse filter criteria," *IEEE Trans. Signal Process.*, vol. 45, pp. 658–672, Mar. 1997.

[27] U. Tureli and P. J. Honan, "Modified high-efficiency carrier estimator for OFDM communications with antenna diversity," in *Proc. 35th Asilomar Conf. Signals, Syst., Comput.*, vol. 2, Pacific Grove, CA, Nov. 2001, pp. 1470–1474.

[28] J.-J. van de Beek and P. O. Börjesson *et al.*, "A time and frequency synchronization scheme for multiuser OFDM," *IEEE J. Sel. Areas Commun.*, vol. 17, pp. 1900–1914, Nov. 1999.

[29] J.-J. van de Beek, M. Sandell, and P. O. Börjesson, "ML estimation of time and frequency offset in OFDM systems," *IEEE Trans. Signal Process.*, vol. 45, pp. 1800–1805, Jul. 1997.

[30] X. Ma, M.-K. Oh, G. B. Giannakis, and D.-J. Park, "Hopping pilots for estimation of frequency-offset and multiantenna channels in MIMO-OFDM," in *Proc. GLOBECOM*, vol. 2, San Francisco, CA, Dec. 2003, pp. 1084–1088.

Yingwei Yao (S'98–M'03) received the Ph.D. degree in electrical engineering from Princeton University, Princeton, NJ, in 2002.

He was a Postdoctoral Researcher with the University of Minnesota, Minneapolis, from 2002 to 2004. Currently, he is an Assistant Professor of Electrical and Computer Engineering with the University of Illinois at Chicago. His research interests include statistical signal processing, wireless communication theory, and wireless networks.

Georgios B. Giannakis (S'84–M'86–SM'91–F'97) received the Diploma in electrical engineering from the National Technical University of Athens, Greece, in 1981. He received the MSc. degree in electrical engineering in 1983, M.Sc. degree in mathematics in 1986, and the Ph.D. degree in electrical engineering in 1986, from the University of Southern California (USC), Los Angeles.

After lecturing for one year at USC, he joined the University of Virginia, Charlottesville, in 1987, where he became a Professor of Electrical Engineering in 1997. Since 1999, he has been with the University of Minnesota, Minneapolis, as a Professor in the Department of Electrical and Computer Engineering, and holds an ADC Chair in Wireless Telecommunications. His general interests span the areas of communications and signal processing, estimation and detection theory, time-series analysis, and system identification, subjects on which he has published more than 200 journal papers, 350 conference papers, and two edited books. Current research focuses on transmitter and receiver diversity techniques for single- and multiuser fading communication channels, complex-field and space–time coding, multicarrier, ultra-wideband wireless communication systems, cross-layer designs, and distributed sensor networks.

Dr. Giannakis is the corecipient of six Best Paper Awards from the IEEE Signal Processing (SP) Society (1992, 1998, 2000, 2001, 2003, and 2004). He also received the Society's Technical Achievement Award in 2000. He co-organized three IEEE-SP Workshops, and guest co-edited four special issues. He has served as Editor in Chief for the IEEE SIGNAL PROCESSING LETTERS, as Associate Editor for the IEEE TRANSACTIONS ON SIGNAL PROCESSING and the IEEE SIGNAL PROCESSING LETTERS, as secretary of the SP Conference Board, as member of the SP Publications Board, as member and vice-chair of the Statistical Signal and Array Processing Technical Committee, and as chair of the SP for Communications Technical Committee. He has served as a member of the Editorial Board for the PROCEEDINGS OF THE IEEE, and the steering committee of the IEEE TRANSACTIONS ON WIRELESS COMMUNICATIONS. He is a member of the IEEE Fellows Election Committee, and has served on the IEEE-SP Society's Board of Governors.